Correlating the Expression and Functional Activity of ABCA4 Disease Variants With the Phenotype of Patients With Stargardt Disease

Fabian Garces,[1] Kailun Jiang,[2] Laurie L. Molday,[1] Heidi Stöhr,[3] Bernhard H. Weber,[3] Christopher J. Lyons,[2] David Maberley,[2] and Robert S. Molday[1,2]

[1]Department of Biochemistry and Molecular Biology, University of British Columbia, Vancouver, British Columbia, Canada
[2]Department of Ophthalmology and Visual Sciences, University of British Columbia, Vancouver, British Columbia, Canada
[3]Institute of Human Genetics, University of Regensburg, Regensburg, Germany

Correspondence: Robert S. Molday, Department of Biochemistry and Molecular Biology, 2350 Health Sciences Mall, University of British Columbia, Vancouver, British Columbia V6T 1Z3, Canada; molday@mail.ubc.ca.

FG and KJ contributed equally to the work presented here and should therefore be regarded as equivalent authors.

Submitted: November 13, 2017
Accepted: April 8, 2018

Citation: Garces F, Jiang K, Molday LL, et al. Correlating the expression and functional activity of ABCA4 disease variants with the phenotype of patients with Stargardt disease. *Invest Ophthalmol Vis Sci*. 2018;59:2305–2315. https://doi.org/10.1167/iovs.17-23364

Purpose. Stargardt disease (STGD1), the most common early-onset recessive macular degeneration, is caused by mutations in the gene encoding the ATP-binding cassette transporter ABCA4. Although extensive genetic studies have identified more than 1000 mutations that cause STGD1 and related ABCA4-associated diseases, few studies have investigated the extent to which mutations affect the biochemical properties of ABCA4. The purpose of this study was to correlate the expression and functional activities of missense mutations in ABCA4 identified in a cohort of Canadian patients with their clinical phenotype.

Methods. Eleven patients from British Columbia were diagnosed with STGD1. The exons and exon-intron boundaries were sequenced to identify potential pathologic mutations in ABCA4. Missense mutations were expressed in HEK293T cells and their level of expression, retinoid substrate binding properties, and ATPase activities were measured and correlated with the phenotype of the STGD1 patients.

Results. Of the 11 STGD1 patients analyzed, 7 patients had two mutations in *ABCA4*, 3 patients had one detected mutation, and 1 patient had no mutations in the exons and flanking regions. Included in this cohort of patients was a severely affected 11-year-old child who was homozygous for the novel p.Ala1794Pro mutation. Expression and functional analysis of this variant and other disease-associated variants compared favorably with the phenotypes of this cohort of STGD1 patients.

Conclusions. Although many factors contribute to the phenotype of STGD1 patients, the expression and residual activity of ABCA4 mutants play a major role in determining the disease severity of STGD1 patients.

Keywords: Stargardt disease, ABCA4, protein expression, phenotype-genotype, functional activity

Stargardt disease (STGD1:MIM 248200) is the most common inherited macular dystrophy affecting 1 in 10,000 people.[1–3] Affected individuals typically show bilateral loss of central vision, impaired color vision, delayed dark adaptation, atrophy of the macula, and accumulation of yellow-white flecks at the level of the RPE.[3–8] The age of onset and disease severity vary widely, but in most cases, STGD1 patients experience a significant reduction in visual acuity in their first or second decade of life and progressive loss in vision during their lifetime.[5,9]

STGD1 is caused by mutations in the gene encoding the ATP-binding cassette (ABC) transporter ABCA4, originally known as ABCR and the Rim protein.[10,11] To date, more than 1000 mutations are known to cause STGD1 and the related ABCA4-associated diseases including a subset of autosomal recessive cone-rod dystrophies and retinitis pigmentosa.[10,12–20] Disease-causing mutations include missense mutations, frameshifts, truncations, small deletions, insertions, and splicing mutations with most being missense mutations encoding amino acid substitutions throughout the protein.

ABCA4 is expressed in rod and cone photoreceptors where it predominantly localizes to the rim region of outer segment disc membranes.[11,21,22] Biochemical studies have shown that ABCA4 actively transports *N*-retinylidene-phosphatidylethanolamine (*N*-Ret-PE), the Schiff-base adduct of retinal and phosphatidylethanolamine (PE), from the lumen to the cytoplasmic leaflet of disc membranes.[23–26] This enables the reduction of all-*trans* retinal and excess 11-*cis* retinal to retinol by retinol dehydrogenase 8 (RDH8), thereby preventing side reactions that produce potentially toxic bisretinoid compounds.[24,27–30]

Although significant progress has been made in identifying disease-causing mutations in *ABCA4*, deciphering genotype-phenotype relationships remains challenging because most patients are compound heterozygous for disease mutations in *ABCA4* and phenotypic variations are found in individuals with the same mutations and in the same family.[31–33] Furthermore, with some exceptions,[23,34–36] analysis of STGD1 has relied on clinical and genetic data while lacking molecular characterization of disease-causing variants. As a result, it remains to be

determined the extent to which the properties of ABCA4 disease variants contribute to the etiology of STGD1 in relation to other factors, such as age, lifestyle, environmental factors, and genetic modifiers. Nonetheless, clinical and genetic studies have provided a thorough assessment of disease-associated mutations in *ABCA4* with respect to population frequency, ethnic groups, age of onset, and severity.[12,13,20,37–39]

In this study, we combine clinical and genetic data with protein expression and functional analysis of disease-associated variants of ABCA4 found in 10 patients in Western Canada diagnosed with STGD1. We also report, for the first time, a novel c.5380G>C/p.Ala1794Pro missense mutation located within the second transmembrane domain of ABCA4, which causes an early onset and severe form of STGD1 in an individual homozygous for this mutation.

Materials and Methods

Clinical Assessment and Mutational Screening of Patients

Individuals in this study were clinically assessed by measuring visual acuity (VA), retina autofluorescence (AF), full-field ERG, spectral domain optical coherence tomography (SD-OCT), intravenous fluorescein angiography (IVFA), slit-lamp biomicroscopy, and tonometry, and their disease stage was categorized according to the Fishman classification (FC) for Stargardt disease.[39,40] In this clinical classification, stage 1 patients typically show parafoveal or perifoveal flecks, pigmentary changes in the macula, and normal ERGs; stage 2 patients exhibit flecks throughout the posterior pole, anterior to the vascular arcades and nasal to the optic disc and relatively normal ERGs but with prolonged dark adaptation; stage 3 patients display diffusely resorbed flecks, choriocapillaris atrophy in the macula, reduced cone or cone and rod ERGs, and central and peripheral field impairment; and stage 4 patients show extensive choroid and RPE atrophy throughout the fundus, decreased ERG cone and rod amplitudes, and moderate to severe peripheral field restriction.

For genotyping, DNA was isolated from 3 to 5 mL of peripheral blood using the Qiagen (Valencia, CA, USA) QIAamp DNA blood Maxi-kit. Mutation testing of all coding exons and the flanking intronic sequences of the *ABCA4, CNGB3,* and *ELOVL4* genes was performed by next-generation sequencing, as described previously.[13] Informed consent was obtained from all individuals and all procedures were approved by the Institutional Ethics Review Board at the University of British Columbia and followed the tenets of the Declaration of Helsinki.

Generation of ABCA4 Mutant Constructs

The cDNA of human *ABCA4*[10,15] engineered to contain a 1D4 tag (TETSQVAPA) at the C-terminus of the protein has been described previously.[41] Missense mutations were generated by PCR-based site-directed mutagenesis. All DNA constructs were verified by Sanger DNA sequencing.

Heterologous Expression Analysis of ABCA4 Variants

Ten-centimeter dishes containing HEK293T cells at 80% to 90% confluency were transiently transfected with 10 μg of pCEP4-ABCA4-1D4 mutant constructs using 1 mg/mL linear polyethyleneimine (PEI), average molecular weight 25,000 Daltons at a 1:3 DNA:PEI ratio for 6 to 8 hours before replacing with fresh media. Forty-eight-hour posttransfection cells were harvested and centrifuged at 2800*g* for 15 minutes. The pellet was resuspended in 100 μL of resuspension buffer (50 mM HEPES, 100 mM NaCl, 5 mM $MgCl_2$, 10% glycerol, pH 7.4). The solution was divided in half and solubilized for 40 minutes in 500 μL of either 3-[(3-Cholamidopropyl)dimethylammonio]-1-propanesulfonate hydrate (CHAPS) solubilization buffer (20 mM CHAPS, 50 mM HEPES, 100 mM NaCl, 5 mM $MgCl_2$, 1 mM dithiothreitol [DTT], 1X ProteinArrest, 10% glycerol, 0.15 mg/mL brain-polar-lipid [BPL], and 0.15 mg/mL 1,2-dioleoyl-sn-glycero-3-phospho-L-ethanolamine [DOPE] [Avanti Polar Lipids, Alabaster, AL, USA], pH 7.4) or SDS solubilization buffer (3% SDS, 50 mM HEPES, 100 mM NaCl, 5 mM $MgCl_2$, 1 mM DTT, 1X ProteinArrest, 10% glycerol, 0.15 mg/ml BPL, and 0.15 mg/mL DOPE, pH 7.4). The samples were then centrifuged at 100,000*g* (TLA110.4 rotor Beckman Optima TL centrifuge [Brea, CA, USA]) and the supernatant was collected. Protein concentration of the supernatant was determined from the absorbance at 280 nm. The samples (7–8 μg of total protein per lane) were resolved on an 8% polyacrylamide gel and transferred onto a polyvinylidene difluoride membrane for Western blotting. Blots were blocked in 1% milk for 60 minutes and subsequently labeled with Rho1D4 mouse monoclonal antibody[42] (1:100 dilution) and rabbit-anti-β-tubulin (1:1000 dilution) as a loading control followed by donkey anti-mouse IgG or donkey anti-rabbit IgG conjugated to IRdye 680 for imaging on an Odyssey Li-Cor imager (Li-Cor, Lincoln, NE). Protein expression levels were quantified based on the intensity of the ABCA4 bands as measured by Western blotting and normalized from the intensity of the bands of the β-tubulin loading control.

Immunofluorescence Microscopy of Transiently Transfected COS-7 Cells

COS-7 cells were transfected with PolyJet (SignaGen, Rockville, MD) reagent according to the manufacturer's guidelines. In brief, COS-7 cells were seeded 24 hours before transfection on six-well plates containing coverslips coated with poly-L-lysine to promote cell adhesion to coverslips. The cells were transfected at 70% to 80% confluency with 1 μg DNA and 3 μL PolyJet for 6 to 8 hours before replacing with fresh media. At 48 hours posttransfection, the cells were fixed with 4% paraformaldehyde in 0.1M phosphate buffer (PB), pH 7.4, and blocked with normal goat serum in 0.2% Triton X-100 and PB for 30 minutes. Primary antibody labeling was carried out for 3 hours using the Rho1D4 antibody against the 1D4-tag and the calnexin rabbit-polyclonal antibody as an endoplasmic reticulum (ER) marker. Secondary labeling was carried out using Alexa-488 goat-anti-mouse (for ABCA4) and Alexa-594 goat-anti-rabbit (for calnexin) for 1 hour. The cells were visualized under a Zeiss (Oberkochen, Germany) LSM700 confocal microscope using a ×40 objective (aperture of 1.3). Images were analyzed using Zeiss Zen software.

Retinoid Binding Assay

Tritiated all-*trans* retinal was prepared by the method of Garwin and Saari[43] with minor modifications.[44] [^{3}H] all-*trans* retinal was mixed with unlabeled all-*trans* retinal to obtain a final concentration of 1 mM and a specific activity of 500 to 1000 dpm/pmol. The binding of [^{3}H] all-*trans* retinal was carried out as previously described.[41] For a typical binding assay, two 150-mm diameter × 25-mm tissue culture dishes of transfected HEK293T cells at 80% to 90% confluency were harvested in 10 mL of Dulbecco's modified Eagle's medium and centrifuged for 15 minutes at 2800*g*. The pellet was resuspended in 100 μL of resuspension buffer (50 mM HEPES, 100 mM NaCl, 5 mM $MgCl_2$, 10% glycerol, pH 7.4) and

solubilized in 3 mL of CHAPS solubilization buffer for 40 to 60 minutes at 4°C as described above. After centrifugation at 100,000*g* for 10 minutes to remove unsolubilized material, the supernatant was divided in half. Each half was incubated with 80 μL of packed Rho1D4-Sepharose-2B affinity matrix equilibrated in column buffer (10 mM CHAPS, 50 mM HEPES, 100 mM NaCl, 5 mM $MgCl_2$, 1 mM DTT, 1X ProteinArrest, 10% glycerol, 0.15 mg/mL BPL, and 0.15 mg/ml DOPE, pH 7.4) and mixed by rotation for 60 minutes at 4°C. The affinity matrix was washed twice with 500 μL of column buffer and mixed with 250 μL of 10 μM [^{3}H] all-*trans* retinal (500 dpm/pmol) in column buffer for 30 minutes at 4°C. The matrix was washed six more times with 500 μL of column buffer. One sample was incubated with 1 mM ATP and the other half was incubated in the absence of ATP for 15 minutes at 4°C. The affinity matrices were washed twice with 500 μL of column buffer and subsequently transferred to an Ultrafree-MC (0.45 um filter) spin column (Millipore, Bedford, MA, USA) followed by another five washes of 500 μL of column buffer. Bound [^{3}H] all-*trans* retinal was extracted with 500 μL of ice-cold ethanol with shaking at 500 rpm for 20 minutes at room temperature and counted in a liquid scintillation counter. Bound ABCA4 was eluted from the Rho1D4-bead matrix with 3% SDS in column buffer and applied to an 8% SDS-polyacrylamide gel for analysis of protein levels by Western blotting. ABCA1, which does not bind retinal,[41] was used as a control to subtract out nonspecific [^{3}H] all-*trans* retinal binding to the affinity matrix.

ATPase Assay

Transfected HEK293T cells (1–2 150 × 25-mm dishes of HEK293T cells at 80%–90% confluency) were solubilized in 3 mL CHAPS solubilization buffer for 40 to 60 minutes at 4°C followed by a 100,000*g* centrifugation for 10 minutes. The supernatant was incubated with 100 μL packed Rho1D4-Sepharose matrix 60 minutes at 4°C. The beads were washed twice with 500 μL column buffer and transferred to an Ultrafree-MC spin column and washed another six times with 500 μL of column buffer. Bound ABCA4 was eluted from the Rho1D4 matrix twice with 100 μL 0.5 mg/mL 1D4 peptide in column buffer. The eluates were pooled and the ABCA4 protein concentration was estimated from the absorbance 280 nm readings. Liposomes consisting of 9.6 mg/mL brain polar-lipid, 2.4 mg/mL DOPE, 0.001% cholesteryl hemisuccinate, 50 mM HEPES, 150 mM NaCl, 5 mM $MgCl_2$, 10% glycerol, 1 mM DTT, 0.5% octyl β-D-glucopyranoside were prepared by bath sonication for 3 to 5 hours at 4°C until turbidity of solution was minimal. ABCA4 eluates were then dialyzed for 24 hours with three 1-L changes of dialysis buffer (50 mM HEPES, 100 mM NaCl, 5 mM $MgCl_2$, 1 mM DTT, 10% sucrose) to remove the detergent.

ATPase assays were carried out using the ADP-GloTM Kinase Assay kit (Promega, Madison, WI, USA) according to the manufacturer's instructions. Reconstituted ABCA4 proteoliposomes were divided into six microcentrifuge tubes containing 15 μL reconstituted protein (~200 ng of ABCA4). One microliter of 0.8 mM all-*trans* retinal (or ATPase buffer alone) was added to half of the reconstituted samples (done in triplicate) to obtain a final concentration of 40 μM all-*trans* retinal and incubated for 15 minutes at room temperature in the dark. After initial incubation period, 4 μL of a 1 mM ATP solution (in ATPase buffer) was added and the samples were incubated at 37°C for 40 minutes. Five microliters of each sample was placed into a well of a 384-well white bottom plate and incubated with 5 μL of ADP-Glo reagent for 60 minutes to stop the ATPase reaction and deplete remaining ATP. Ten microliters of ADP-Glo detection reagent was added and samples were incubated for 60 minutes at room temperature before luminescence readings. Standard ADP:ATP solutions were used to generate a standard curve and calculate the amount of ATP hydrolyzed. Luminescence was measured with a microtiter plate reader. Reconstituted ABCA4 samples were loaded onto an 8% acrylamide gel along with BSA standards to calculate the amount of ABCA4 in each sample. The ATPase-deficient mutant ABCA4-MM in which the lysine residues in the Walker A motif of nucleotide binding domain 1 (NBD1) and nucleotide binding domain 2 (NBD2) were substituted for methionine was used to subtract background luminescence.[45]

Results

Genetic Screening of STGD1 Patients

Eleven individuals from British Columbia, Canada, with impaired vision and clinical features characteristic of STGD1 were recruited for this study. The patients were screened for mutations in the *ABCA4*, *CNGB3,* and *ELOVL4* genes. Sequence variations in the *ABCA4* were identified in 10 patients, 2 of which (c.213dupG and c.5380G>C) have not been previously reported (Table 1). Seven patients had two mutations, including one patient who was homozygous for the novel c.5380G>C, p.Ala1794Pro mutation. A mutation in only one *ABCA4* allele was found in two patients. One other individual had two mutations, p.Leu541Pro and p.Ala1038Val. These two mutations are commonly found together as a complex mutation c.[1622T>C;3113C>T]/p.[Leu541Pro;Ala1038Val] in the German population.[12,36,38] One patient (patient 7) with a STGD1 phenotype had no detectable mutations in the *ABCA4* gene and therefore was excluded from our study. No disease-associated mutations were found in *CNGB3* encoding the cone cyclic nucleotide-gated channel B3 subunit or *ELOVL4* encoding the elongation of very long chain fatty acids protein 4 in any of the patients examined in this study.

Clinical Assessment of STGD1 Patients

Patient 3, 28 years old, carrying the c.214G>A/p.Gly72Arg and c.5882G>A/p.Gly1961Glu mutations is legally blind with VA of 20/200 and stage 3 FC. This patient displayed considerable foveal RPE atrophy accounting for poor VA (Fig. 1). The 22-year-old younger sibling (patient 2; Table 1) also carried these mutations, but showed a VA of 20/30 and stage 1 FC. The difference in VA between the two siblings with identical genotype may be due to the progressive nature of the disease and/or familial variation. The mother (patient 1) with normal 20/20 VA and no signs of STGD1 was a carrier of the p.Gly1961Glu mutation consistent with the recessive nature of STGD1 (Fig. 1). At a genetic level, both the p.Gly1961Glu and p.Gly72Arg are classified as pathogenic and likely pathogenic, respectively, consistent with the STGD1 disease assessment (see Table 1). Functional analysis of p.Gly72Arg given below clearly indicates that this missense mutation is pathogenic (Table 2).

Patient 4, a 30-year-old individual with the deleterious c.213dupG/p.Ile73Asnfs*26 frameshift mutation and the c.1654G>A/p.Val552Ile missense mutation, displayed mild STGD1 with stage 2 FC and 20/30 VA. The p.Ile73Asnfs*26 mutation is classified as a pathogenic mutation, whereas the p.Val552Ile mutation is classified as likely neutral. Biochemical analysis of the p.Val552Val, however, suggests that this is a mild mutation at a functional level consistent with the clinical assessment of patient 4 (see Discussion section for additional information).

Investigative Ophthalmology & Visual Science

Table 1. Genotype and Phenotype Characteristics of STGD1 Patients Harboring *ABCA4* Mutations

Patient	Age	Mutation 1	Category*	Mutation 2	Category*	Visual Acuity	FC†
2	22	Exon 3: c.214G>A, p.(Gly72Arg)[12]	UV4	Exon 42: c.5882G>A, p.(Gly1961Glu)[12]	UV5	20/30	Stage 1
3	28	Exon 3: c.214G>A, p.(Gly72Arg)[12]	UV4	Exon 42: c.5882G>A, p.(Gly1961Glu)[12]	UV5	20/200	Stage 3
4	30	Exon 3: c.213dupG, p.(Ile73Aspfs*26)‡	UV5	Exon 12: c.1654G>A, p.(Val552Ile)[50]	UV2	20/30	Stage 2
5	11	Exon 38: c.5380G>C, p.(Ala1794Pro)‡	UV4	Exon 38: c.5380G>C, p.(Ala1794Pro)‡	UV4	20/200	Stage 3
6	55	Exon 45: c.6229C>T, p.(Arg2077Trp)[12]	UV4	-		20/40	Stage 3
8	13	c. [1622T>C; 3113C>T], p. [Leu541Pro; Ala1038Val][20,36]	UV5	-		20/200	Stage 4
9	30	Exon 22: c.3272G>A, p.(Gly1091Glu)[55]	UV4	Intron 40: c.5714+5G>A, p.[=,Glu1863Leufs*33][12,54]	UV5	20/160	Stage 4
10	36	Intron 38: c.5461-10T>C, p.(Thr1821Aspfs*6)[54]	UV5	Exon 44: c.6079C>T, p.(Leu2027Phe)[55]	UV5	20/200	Stage 4
11	45	Intron 8: c.1099+1G>C, p.(?)[56]	UV5	Exon 10: c.1343T>A, p.(Met448Lys)[57]	UV4	20/400	Stage 4
12	63	Exon 27: c.4069G>A, p.(Ala1357Thr)[58]	UV4	-		20/400	Stage 3

Patient 1, a carrier of the c.5882G>A, p.(Gly1961Glu) mutation, is the parent of patients 2 and 3 and does not have STGD1. Patient 7 with STGD1 and FC 3 did not have any detectable mutations in the *ABCA4* gene and therefore was not included in our study. (=), wild type.

* UV1, neutral; UV2, likely neutral; UV3, unknown pathogenicity; UV4, likely pathogenic; UV5, pathogenic. Based on Refs. 13, 20.

† FC, as described in Material and Methods and Refs. 39, 40.

‡ This study.

Patient 8, a 13-year-old individual carrying two mutations, the p.Leu541Pro and p.Ala1038Val, most likely as a complex allele, had an early disease onset with 20/200 VA and stage 4 FC (Table 1). Previous reports have documented the severity and early age of onset associated with the p.[Leu541Pro;Ala1038Val] complex variant.[36,38] Our screening studies failed to detect an additional mutation in *ABCA4* in patients 6, 8, or 12.

Patients 9, 10, and 11, all carrying one deleterious splice-site mutation and a missense mutation (c.5714+5G>A/p.Gly1091Glu; c.5461–10T>C/p.Leu2027Phe; c.1099+1G>C/p.Met448Lys), had advanced STGD1 with stage 4 FC, and poor VA (Table 1). The missense variants were classified as pathogenic or likely pathogenic by genetic analysis (Table 1).

Patient 5, an 11-year-old child, had severe STGD1 with VA of 20/200, bilateral bull's eye maculopathy with dull fovea reflex, peripheral flecks, bilateral dark choroid with central RPE disruption, paracentral pisciform lesions on fluorescence angiography, and central outer retinal disruption as visualized by SD-OCT (Fig. 1). The FC of this patient is stage 3 despite poor VA and advanced RPE atrophy because the ERG measurements displayed severely reduced cone response but near normal rod response. Sequence analysis indicated that this patient was homozygous for a novel p.Ala1794Pro missense mutation classified genetically as likely pathogenic (Fig. 1, Table 1). This is confirmed by severely reduced expression and functional activity of this mutant as described in the subsequent sections and Table 2.

Expression and Localization of ABCA4 Disease Variants in Culture Cells

The distribution of the 11 missense mutations found in our STGD1 patient cohort within the current topological model for ABCA4[29,46] is presented in Figure 2. Four missense mutations were found within the exocytoplasmic domain 1, three in or NBD1, three in NBD2, and one mutation within transmembrane segment 11 of transmembrane domain 2.

To determine the effect of disease-causing mutations on ABCA4, we first investigated the level of expression and cellular distribution of the 11 variants and wild-type (WT) ABCA4 transiently expressed in mammalian culture cells. This was carried out by comparing the solubility of the proteins in CHAPS relative to SDS and visualizing the subcellular localization of these mutants in transfected cells by immunofluorescence microscopy.

CHAPS is a mild detergent widely used to solubilize and purify membrane proteins in a native-like state for functional characterization.[21,41] Denatured proteins typically aggregate in CHAPS and can be effectively removed by high-speed centrifugation. In contrast, SDS is a strong detergent that solubilizes both native and denatured proteins. It can be used to determine total expression of proteins (e.g., both native and denatured protein). The degree of detergent solubilization of the ABCA4 mutants by CHAPS and SDS is shown in Western blots in Figure 3A and quantified in Figure 3B. All variants expressed at similar levels as determined by solubilization with SDS. In CHAPS detergent, however, five variants (p.Gly72Arg, p.Met448Lys, p.Leu541Pro, p.Val552Ile, and p.Gly1961Glu) solubilized at levels broadly similar to WT ABCA4; two mutants (p.Ala1038Val and p.Gly1091Glu) solubilized at 70% WT level, and the remaining four mutants (p.Ala1357Thr, p.Ala1794Pro, p.Leu2027Phe, and p.Arg2077Trp) solubilized at or below 50% of the WT level as shown in Figure 3B.

The distribution of ABCA4 variants in transiently transfected COS-7 cells was visualized by immunofluorescence microscopy (Fig. 4). As previously reported,[41,45] WT ABCA4 showed a punctate staining pattern characteristic of intracellular vesicle-like structures containing calnexin with some evidence of ER

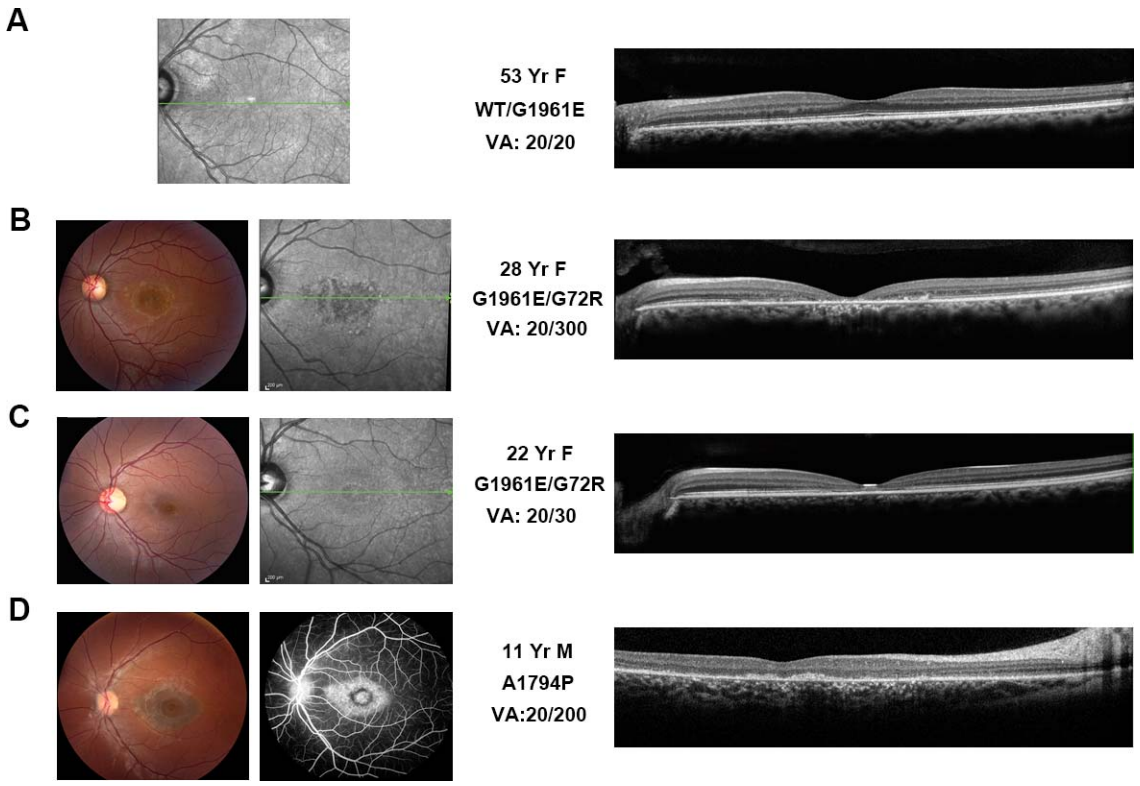

Figure 1. Representative clinical features of STGD1 patients examined in this study. *Left*: Color fundus (CF) images and retinal AF. *Right*: OCT images. (**A**) Patient 1, a carrier of the p.Gly1961Glu mutation (WT/G1961E), showing normal CF, AF, and OCT images. (**B**) and (**C**) Patients 2 and 3, two siblings with identical genotype p.Gly1961Glu/p.Gly72Arg (G1961E/G72R); and (**D**) patient 5, an individual homozygous for the p.Ala1794Pro (A1794P) mutation. AF illustrates lipofuscin accumulation in all STGD1 patients but not the carrier individual. OCT of patients shows atrophy of the RPE cells around the fovea of STGD1 with the most severe degeneration for patient 5. (**D**) (*Left*) shows a fluorescein angiogram alongside of a fundus photograph of a dark choroid.

reticular staining. Seven disease variants (p.Gly72Arg, p.Met448Lys, p.Leu541Pro, p.Val552Ile, p.Ala1038Val, p.Gly1091Glu, and p.Gly1961Glu) showed similar calnexin-associated vesicle structures and reticular ER staining (Fig. 4). A distinctive reticular expression pattern was most evident for p.Ala1357Thr, p.Ala1794Pro, p.Leu2027Phe, and p.Arg2077Trp disease variants with little or no vesicular structures. In general, disease variants that expressed at or near WT ABCA4 levels as determined by CHAPS solubilization exhibited vesicular staining, whereas lower-expressing mutants exhibited primarily a reticular staining pattern (Table 2), indicative of protein misfolding and ER retention by the quality control system of the cell.

Functional Analysis of ABCA4 Disease Variants

The functional properties of the ABCA4 variants were determined by measuring *N*-Ret-PE substrate binding in the absence of ATP and loss in binding upon addition of ATP,[26,41] and determining the basal and *N*-Ret-PE stimulated ATPase activity.[23,25,34,47] All-*trans* retinal was used in these assays because in the presence of PE the aldehyde group of all-*trans* retinal reacts reversibly with the primary amine group of PE to form the substrate *N*-Ret-PE.[26,47] For these studies, WT and ABCA4 variants were solubilized in CHAPS and immobilized on an immunoaffinity column. Figure 5A shows the ABCA4 variants after elution from the column confirming the purity of the proteins.

The binding profile of *N*-Ret-PE to ABCA4 variants immobilized on an immunoaffinity matrix is shown in Figure 5B. In the absence of ATP, *N*-Ret-PE binds strongly to WT ABCA4.[26] More than 95% of *N*-Ret-PE binding is abolished by the addition of 1 mM ATP. ABCA4 mutants showed variable substrate binding in the absence and presence of ATP. Generally, they could be divided into three groups: group 1 (p.Val552Ile, p.Gly1091Glu, p.Ala1357Thr) showed similar substrate binding properties as WT ABCA4; group 2 (p.Met448-Lys,p.Ala1038Val, p.Ala1794Pro, and p.Leu2027Phe) showed a significant reduction in substrate binding in the absence of ATP (35% or lower compared with WT ABCA4) with a further reduction in substrate binding in the presence of ATP; and group 3 (p.Gly72Arg, p.Leu541Pro, p.Gly1961Glu, p.Arg2077Trp) showed significantly reduced substrate binding that was insensitive to ATP.

Next, we measured the effect of disease-associated mutations on the ATPase activity of ABCA4. WT and ABCA4 variants were solubilized in CHAPS, purified by immunoaffinity chromatography, and subsequently reconstituted into PE-containing liposomes at similar protein concentrations. The ATPase activity of the mutants in the presence and absence of *N*-Ret-PE substrate is shown in Figure 6A, 6B. As previously reported,[25,47] addition of 40 μM all-*trans* retinal to WT ABCA4 resulted in a 1.8- to 2.5-fold increase in ATPase activity (Fig. 6). The ATPase activity of the mutants was measured at the same protein concentration as WT ABCA4 to determine the effect of the mutation on the functional activity of ABCA4. Five mutants (p.Val552Ile, p.Ala1038Val, p.Ala1357Thr, p.Ala1794Pro, and p.Leu2027Phe) showed reduced basal ATPase activity relative to WT ABCA4 (~40%–85%), but this activity was stimulated 1.6- to 3.0-fold by the addition of all-*trans* retinal. On the other hand, p.Gly72Arg, p.Met448Lys, p.Leu541Pro, p.Gly1091Glu,

Table 2. Expression and Functional Activities of ABCA4 Missense Mutations Identified in the STGD1 Patients

Variant	Cellular Localization	Relative Solubility ± SD	Relative N-Ret-PE Binding ± SD Without ATP	Relative N-Ret-PE Binding ± SD With ATP	Relative ATPase Basal Activity ± SD	Relative Retinal-Stimulated ATPase Activity ± SD	Predicted Effect of the Mutation
WT	Vesicles	100	100	6 ± 5	100	209 ± 40	Normal
G72R	Vesicles	97 ± 16	6 ± 7	8 ± 11	42 ± 19	50 ± 14	Severe
M448K	Vesicles	92 ± 13	33 ± 18	14 ± 12	46 ± 1	62 ± 5	Severe
L541P	Vesicles	100 ± 17	7 ± 7	5 ± 4	59 ± 23	61 ± 18	Severe
V552I	Vesicles	93 ± 11	102 ± 26	4 ± 4	85 ± 13	174 ± 13	Mild
A1038V	Vesicles	71 ± 16	33 ± 15	7 ± 4	65 ± 8	108 ± 14	Moderate
G1091E	Vesicles	73 ± 13	86 ± 6	23 ± 4	41 ± 20	58 ± 25	Moderate
A1357T	ER	55 ± 19	108 ± 11	14 ± 6	39 ± 9	127 ± 36	Moderate
A1794P	ER	50 ± 15	29 ± 13	9 ± 6	76 ± 10	125 ± 15	Severe
G1961E	Vesicles	102 ± 18	36 ± 19	38 ± 22	12 ± 10	13 ± 10	(Mild)*
L2027F	ER	44 ± 15	26 ± 4	11 ± 3	54 ± 19	108 ± 22	Severe
R2077W	ER	52 ± 14	22 ± 7	18 ± 5	31 ± 7	34 ± 9	Severe

* G1961E mutation appears mild when this variant is retained in the membrane based on expression studies and consistent with the relatively mild phenotype of individuals homozygous for this mutation. However, after detergent solubilization, the variant is devoid of functional activity, including N-Ret-PE binding and ATPase activity. Detergent solubilization may adversely affect the functional activities of this mutant.

p.Gly1961Glu, and p.Arg2077Trp variants showed drastically reduced basal activity with little or no substrate stimulation.

To more directly evaluate the expression and function of the p.Ala1794Pro variant, we transfected HEK293T cells separately with WT *ABCA4* and the p.Ala1794Pro mutant cDNAs at similar levels. After solubilization in CHAPS buffer, the samples were subjected to high-speed centrifugation and the supernatant was reconstituted into liposomes for analysis of its basal and substrate activated ATPase activity. As shown in Figure 6C, the p.Ala1794Pro had a significantly reduced activity due largely to the low expression of this variant. These studies indicate that only a small fraction of the p.Ala1794Pro mutant folds into a functionally active protein and correlates well with the phenotype of patient 5.

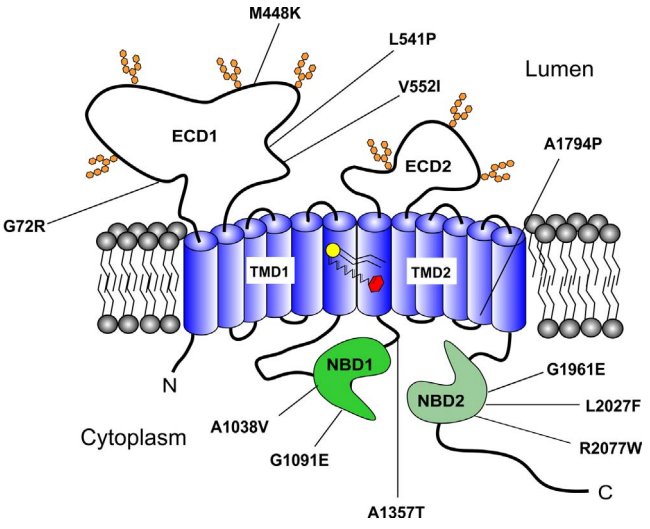

Figure 2. Topological model of ABCA4[46] showing the location of missense mutations associated with Stargardt disease examined in this study. Amino acids are shown as single letters, where G is Gly; R, Arg; M, Met; K, Lys; L, Leu; P, Pro; V, Val; I, Ile; A, Ala; E, Glu; F, Phe; W, Trp; and T, Thr. ABCA4 is organized into two nonequivalent tandem halves with each half consisting of an exocytoplasmic domain (ECD), nucleotide binding domain (NBD), and a transmembrane domain (TMD) with six transmembrane segments. The transport substrate *N*-Ret-PE is shown within the TMDs with transport from the exocytoplasmic (Lumen) to the cytoplasmic leaflet of the disc membrane.

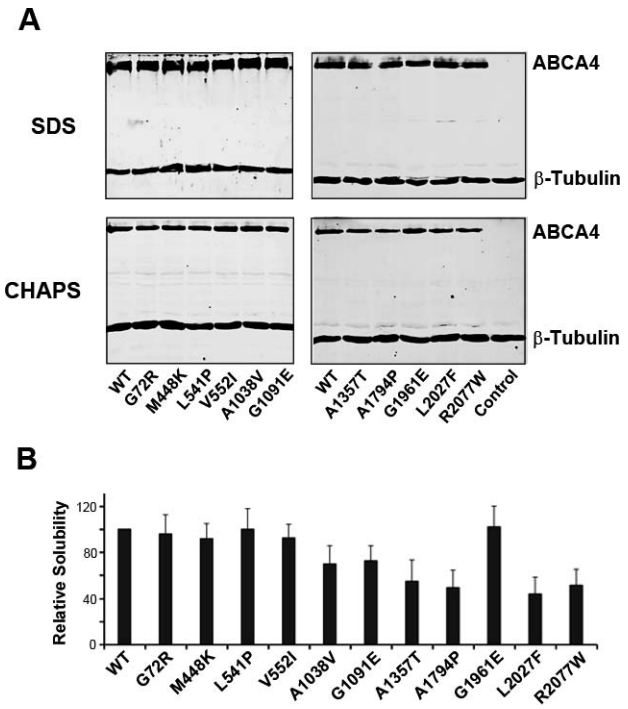

Figure 3. Relative solubility of ABCA4 variants in transiently transfected HEK293T cells. Transfected HEK293T cells were solubilized using either the mild detergent CHAPS or the strong denaturing detergent SDS. The cell lysates were subjected to high-speed centrifugation to remove unsolubilized material and the supernatants (7–8 μg protein per lane) were resolved by SDS gel electrophoresis and subsequently analyzed on Western blots labeled for ABCA4. (**A**) Western blots labeled with the rho 1D4 antibody to epitope-tagged ABCA4; β-tubulin was used as a loading control to normalize the amount of protein loaded across all samples. (**B**) Quantification of the Western blots of CHAPS solubilized ABCA4 relative to SDS solubilized ABCA4. Graph showing the ratio of ABCA4 variants in CHAPS versus SDS relative to WT levels as determined from Western blots. Data are the average ± SD for $n = 4$ independent experiments.

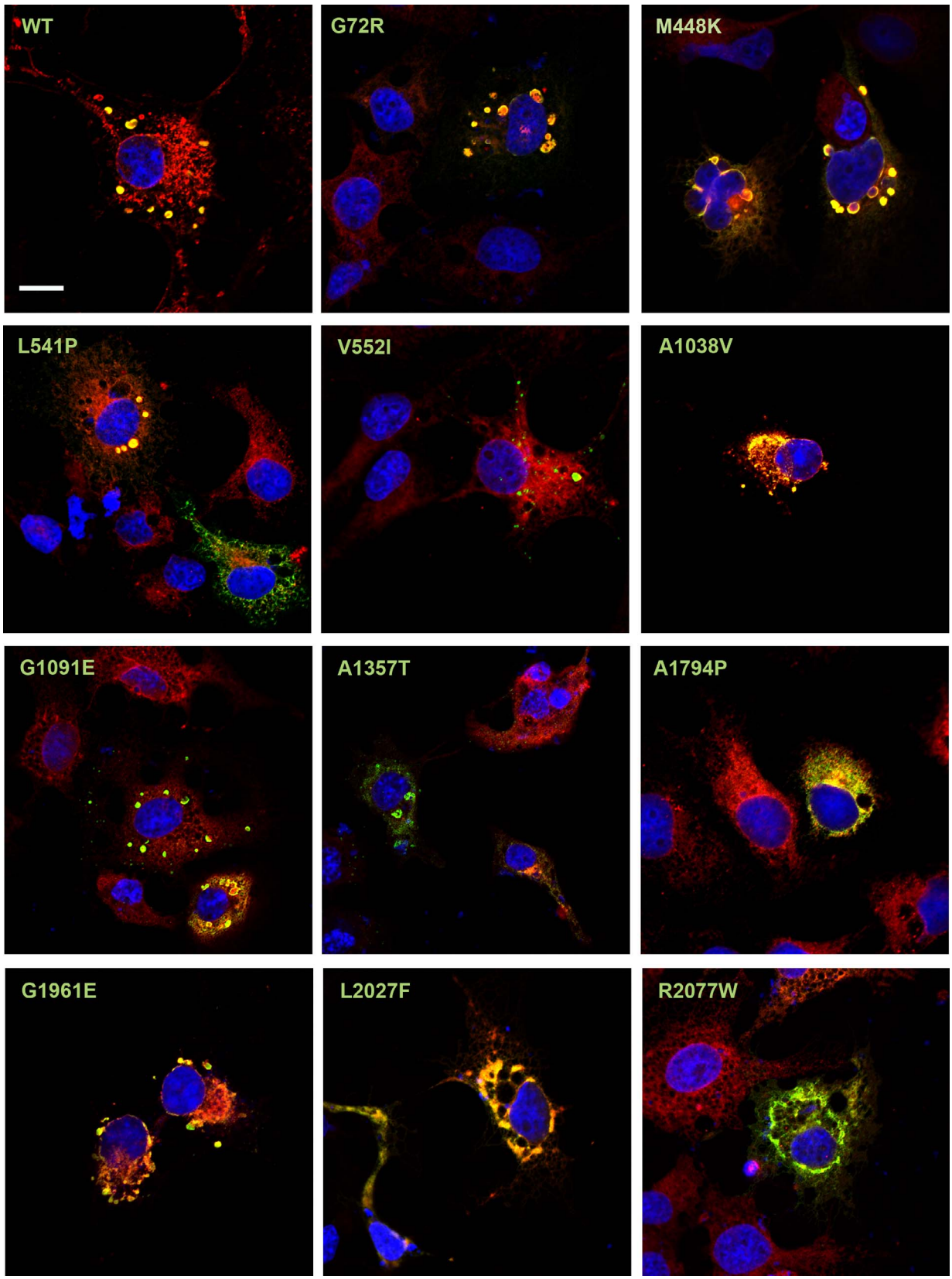

Figure 4. Cellular localization of ABCA4 variants. COS7 cells were transfected with mutant constructs and double-labeled for ABCA4 (*green*) and the ER marker calnexin (*red*) for visualization by confocal scanning microscopy. The prevalence of punctate staining characteristic of a vesicular structure is evident for WT ABCA4. The variants showed either punctate staining together with reticulum staining or primarily reticulum staining as in A1794P, L2027F, and R2077W. The cells were counterstained with 4′,6-diamidino-2-phenylindole (DAPI) nuclear stain (*blue*). *Scale bar*: 10 μm.

Investigative Ophthalmology & Visual Science

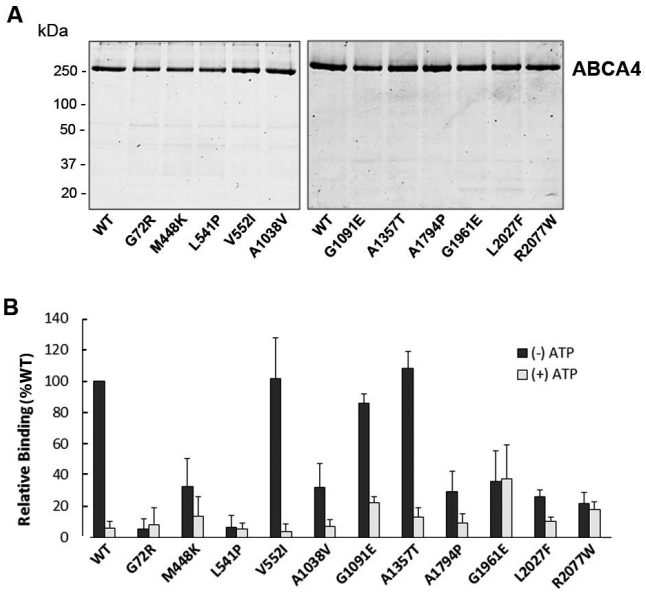

FIGURE 5. Purification and *N*-Ret-PE binding to ABCA4. ABCA4 variants from transfected HEK293T cells were purified on a rho 1D4-immunoaffinity column. (**A**) Coomassie blue–stained SDS gels of WT and ABCA4 variants purified by immunoaffinity chromatography. (**B**) Binding of *N*-Ret-PE to ABCA4 variants in the absence and presence of ATP. *N*-Ret-PE binding was normalized to WT ABCA in the absence of ATP. Data are the average ± SD for $n \geq 3$ independent experiments.

DISCUSSION

STGD1, like most other inherited retinal degenerative diseases, is a highly heterogeneous disorder at both a clinical and genetic level. This is evident in our cohort of patients who show wide variation in phenotypes and genotypes. Phenotypic variation extended from early disease onset with poor VA and evidence of macular atrophy to patients who develop STGD1 well into their adulthood and whose symptoms, including VA, remain relatively mild. Genetic variations included splice-site, frameshift, and missense mutations resulting in amino acid substitutions in various domains of ABCA4 (Fig. 2). In agreement with previous large genetic screens, we identified two mutations in approximately 65% of our patients, one mutation in approximately 25% of the patients, and no mutations in one patient (10%). As discussed elsewhere,[19] the missing disease-causing mutations in patients diagnosed with STGD1 may be due to mutations in noncoding regions of ABCA4 not sequenced in this study, mutations in other genes that can result in phenotypes similar to STGD1, or hypomorphic alleles overlooked in most genetic screens.[19]

In addition to variation in clinical and genetic traits, our studies showed considerable variation in the extent of expression and functional activity of the missense variants as summarized in Table 2. Some mutants expressed at or near WT ABCA4 levels when assayed after mild detergent solubilization, including p.Gly72Arg, p.Met448Lys, p.Leu541Pro, p.Gly1961Glu, and p.Val552Ile, whereas others showed significant reduction in expression, including p.Ala1357Thr, p.Ala1794Pro, p.Leu2027Phe, and p.Arg2077Trp. Variation in *N*-Ret-PE binding and ATPase activity was also observed. Two mutants, p.Val552Ile and p.Ala1357Thr, showed *N*-Ret-PE binding and release by ATP at levels similar to WT ABCA4, whereas other mutants, such as p.Gly72Arg, p.Met448Lys, p.Leu541Pro, and p.Arg2077Trp, showed diminished substrate binding in the presence and absence of ATP. Likewise, basal and retinal activated ATPase activity varied widely with p.Val552Ile, showing almost WT-like activity, and other mutants, including p.Gly72Arg, p.Leu541Pro, p.Gly1961Glu, and p.Arg2077Trp, showing significantly reduced basal activity and little, if any, substrate-stimulated activity.

A main focus of this study was to correlate the expression and functional activity of missense mutations identified in our cohort of STGD1 patients with the clinical phenotypes. Patient 5, homozygous for the p.Ala1794Pro mutation, offers a unique opportunity to directly compare the properties of this ABCA4 variant with the disease severity. Half of the p.Ala1794Pro mutant expressed in HEK293T cells failed to solubilize in CHAPS. Immunofluorescence studies further indicated that most of the p.Ala1794Pro mutant was retained in the ER. These results suggest that a large fraction of p.Ala1794Pro is present in a highly misfolded, aggregated state. Interestingly, the fraction that does solubilize in CHAPS displays *N*-Ret-PE binding and ATPase activity, but at a significantly lower level than WT ABCA4 (Table 2). Combination of low expression and reduced functional activity, as shown in Figure 6C, indicates that only a small fraction of this mutant protein is potentially capable of transporting *N*-Ret-PE across membranes consistent with the severe phenotype of this patient. The inability to clear *N*-Ret-PE and retinal from disc membranes gives rise to the production of bisretinoids that accumulate in RPE cells as evident in the fundus photographs and dark choroid observed for patient 5 (Fig. 2). This in turn leads to degeneration of central RPE and photoreceptor cells, and the early onset and severe phenotype displayed by this patient. The alanine1794 residue is predicted to reside within transmembrane segment 11 of ABCA4 (Fig. 2) based on the topological model of ABCA4[46] and supported by the recent structure of ABCA1,[48] an ABC lipid transporter which is more than 50% identical in sequence to ABCA4. Substitution of an alanine with a proline likely disrupts the α-helical conformation of transmembrane segment 11, resulting in significant misfolding of ABCA4 and retention in the ER of photoreceptor cells. In another study, substitution of alanine 1794 with aspartic acid (p.Ala1794Asp) has been reported to be a STGD1 disease-causing mutation.[49] In this case, the negatively charged aspartic acid residue within transmembrane segment 11 also likely affects the protein folding leading to reduced expression and functional activity of ABCA4 and a STGD1 phenotype.

Patient 4 with an early frameshift mutation in one allele and a downstream p.Val552Ile mutation in the second allele has a mild form of STGD1. Because the frameshift mutation is likely to result in a null allele, any residual functional activity of ABCA4 would arise from ABCA4 harboring the p.Val552Ile missense mutation. Our in vitro studies showing that the p.Val552Ile variant expresses at close to WT levels, exhibits normal *N*-Ret-PE binding properties, and has only a modest reduction in ATPase activity (Table 2) are consistent with the mild disease phenotype of patient 4. Another study has also reported that the p.Val552Ile mutation is associated with a STGD1 disease phenotype.[50] However, in silico predictions on the pathological relevance of this mutation have been variable.[20,13] On the basis of allele frequencies in controls versus patients, it has been argued that the p.Val552Ile is most likely benign.[20] At a protein level, a hydrophobic amino acid residue valine is replaced with another hydrophobic residue isoleucine. Accordingly, this substitution would be predicted to have only a marginal impact on ABCA4 protein structure and function. However, valine at position 552 of ABCA4 is invariable among vertebrate species, including other mammals, chicken, *Xenopus*, and Japanese puffer fish (*Takifugu rubripes*), attesting to the likely importance of valine at this position. Collectively, these studies suggest that the p.Val552Ile is a mild mutation in which the pathogenicity may only be displayed in selected cases. More specifically, the p.Val522Ile

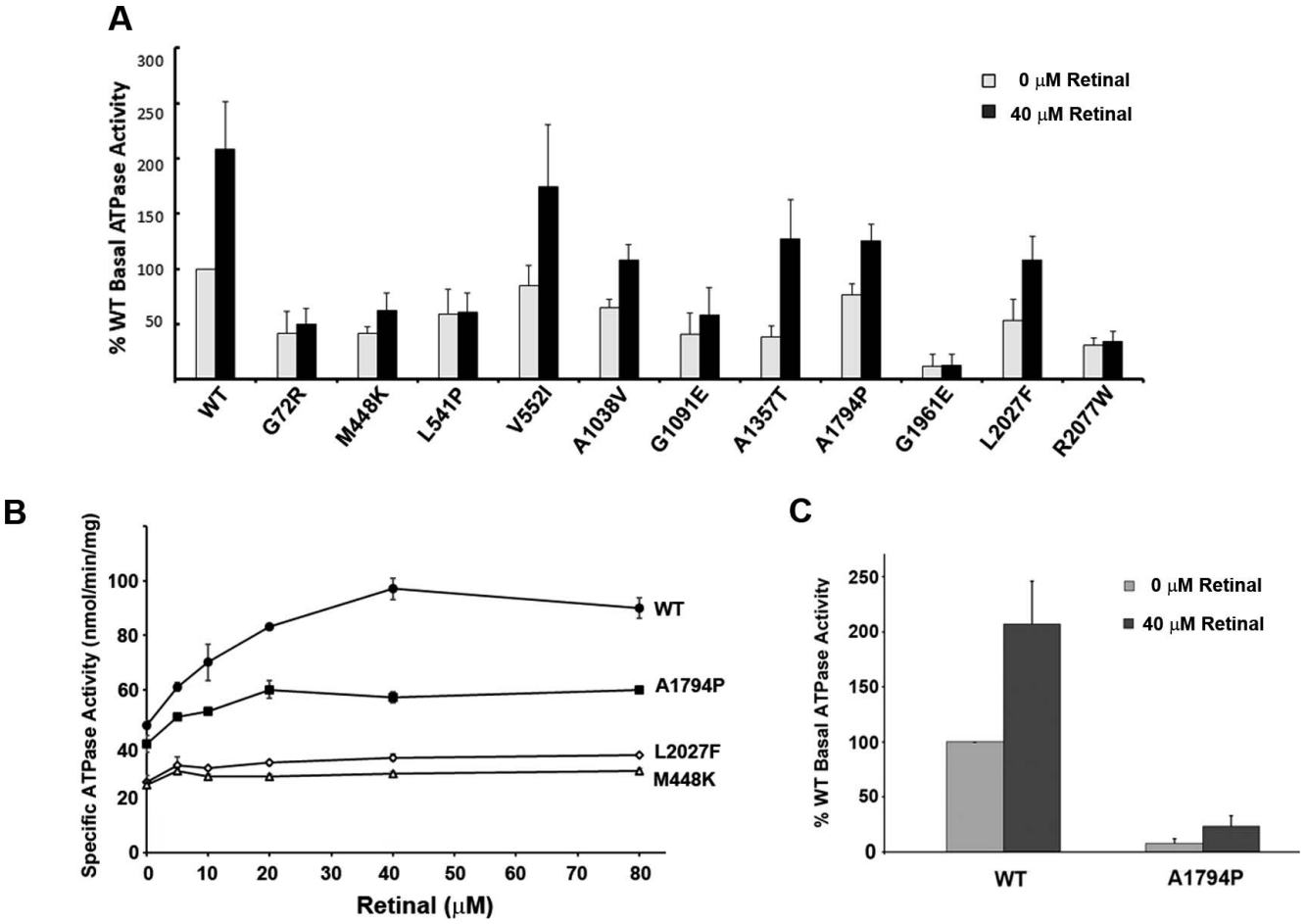

FIGURE 6. ATPase activity of ABCA4 variants. The ATPase activity of immunopurified and reconstituted ABCA4 variants was measured in the presence or absence of all-*trans* retinal. (**A**) Quantification of the basal and retinal-stimulated ATPase activity of ABCA4 variants normalized to WT basal ATPase activity. ATPase assays were carried out using similar concentrations of purified ABCA4. Data expressed as an average ± SD for $n \geq 3$ independent experiments. (**B**) Representative curves of specific ATPase activity as a function of all-*trans* retinal concentration for WT and ABCA4 variants. (**C**) Relative basal ATPase activity of WT and A1794P using equal amounts of transfected HEK293T cells. Data expressed as an average ± SD. Measurements were done in triplicate.

would display a mild STGD1 phenotype when combined with a null allele as in the case of patient 4 or a missense mutation with little or no activity such as the p.Asn965Ser mutation,[37,51] but would not display a disease phenotype in a patient homozygous for this mutation or patients in which this mutation is combined with a mutation that shows significant ABCA4 function because under these circumstances sufficient ABCA4 activity would be realized to prevent the accumulation of toxic retinoids.

The ATPase activity of two disease-associated variants (p.Leu541Pro and p.Ala1038Val) expressed in culture cells have been described previously.[34,36] In our study, the p.Leu541Pro expressed at WT levels in HEK293T cells, but was largely devoid of *N*-Ret-PE binding activity and displays low basal ATPase activity that is not activated by retinoid substrate. These results are in line with previous ATPase activity studies.[34,36] In contrast, the p.Ala1038Val variant has reduced expression (~70% WT), but displays retinal-stimulated ATPase activity and retinal binding activity, although at a lower level than WT. Two previous studies differed in the functional assessment of the p.Ala1038Val variant with one study reporting little if any activity,[34] and another study demonstrating a relatively high level of activity.[36] Our data are consistent with the latter showing significant activity. These mutants are most commonly present as a complex allele.[20] Biochemical studies indicate that both mutations contribute to the loss in function of p.[Leu541Pro;Ala1038Val] ABCA4, but the p.Leu541Pro mutation is the major contributor to the severe pathogenicity associated with this complex mutation. A similar conclusion was derived from the knockin mouse studies of Zhang et al.[36] and genetic analysis of Cornelis et al.[20]

The p.Gly1961Glu variant is another well-studied mutation found in our cohort of STGD1 patients. It is the most common mutation found in STGD1 patients, although its frequency varies between ethnic populations and geographical origins. Previous studies of homozygous and compound heterozygous patients with the p.Gly1961Glu mutation indicate that it is most often associated with a milder, late-onset retinal disease phenotype with individuals typically displaying central macula atrophy, the absence of a dark choroid, and normal full-field ERGs.[52] Two siblings in our cohort had the p.Gly1961Glu mutation in association with the p.Gly72Arg mutation, with one sibling exhibiting a mild-moderate phenotype. The p.Gly72Arg variant expressed at WT levels, but was deficient in *N*-Ret-PE binding and substrate-dependent ATPase activity, indicating that this mutation severely affects ABCA4 function. The p.Gly1961Glu mutation also expressed at WT levels, but displayed a loss in *N*-Ret-PE binding and ATPase activity. The discrepancy between the mild phenotype generally displayed by individuals with p.Gly1961Glu and the severe loss in

Investigative Ophthalmology & Visual Science

function observed in the in vitro studies described here and in a previous report[34] requires further study. However, it is possible that the loss in function exhibited by the p.Gly1961-Glu mutant arises from the effect of detergent solubilization on the functional activity of this variant. In this instance, CHAPS detergent may irreversibly denature the p.Gly1961Glu ABCA4 variant, resulting in the loss in activity. If this is the case, the p.Gly1961Glu variant would be predicted to show significant activity in an in vitro or in vivo assay that does not require detergent solubilization. Such activity assays have yet to be developed. The late-onset relatively mild phenotype of our patients with p.Gly1961Glu may result from residual functional activity of membrane-bound ABCA4 harboring this mutation.

Last, patients 9 to 11 were found to have a splice-site mutation in one allele and a missense mutation in the other allele. The effect of the splice mutations on residual expression of full-length *ABCA4* has been recently studied for two of these mutations (c.5461-10T>C and c.5714+5G>A).[53,54] The c.5461-10T>C mutation causes the skipping of exon 39 or 39/40 resulting in no full-length transcript.[54] On the other hand, the c.5714+5G>A resulted in approximately 40% normally spliced *ABCA4* mRNA. The missense mutations in the other allele (p.Gly1091Glu, p.Leu2027Phe, or p.Met448Lys), which significantly reduces the expression and/or functional activity of ABCA4 as measured in our in vitro assays, is consistent with the relatively severe phenotype found in these patients.

In conclusion, biochemical analyses of ABCA4 variants harboring missense mutations correlate well with the disease phenotype of our STGD1 patients. Although many factors contribute to the phenotype of STGD1 patients, the expression of ABCA4 mutants and the existence of at least some functional activity play an important role in determining the severity of STGD1.

Acknowledgments

Supported in part by grants from the National Institutes of Health (EY002422) and Canadian Institutes of Health Research (PJT-148649) to RSM.

Disclosure: **F. Garces**, None; **K. Jiang**, None; **L.L. Molday**, None; **H. Stöhr**, None; **B.H. Weber**, None; **C.J. Lyons**, None; **D. Maberley**, None; **R.S. Molday**, None

References

1. Gelisken O, De Laey JJ. A clinical review of Stargardt's disease and/or fundus flavimaculatus with follow-up. *Int Ophthalmol*. 1985;8:225–235.
2. Stargardt K. Uber familiare, progressive degeenration under makulagegend des augen. *Albrecht von Graefes Arch Ophthalmol*. 1909;71:534–550.
3. Weleber RG. Stargardt's macular dystrophy. *Arch Ophthalmol*. 1994;112:752–754.
4. Kang Derwent JJ, Derlacki DJ, Hetling JR, et al. Dark adaptation of rod photoreceptors in normal subjects, and in patients with Stargardt disease and an ABCA4 mutation. *Invest Ophthalmol Vis Sci*. 2004;45:2447–2456.
5. Rotenstreich Y, Fishman GA, Anderson RJ. Visual acuity loss and clinical observations in a large series of patients with Stargardt disease. *Ophthalmology*. 2003;110:1151–1158.
6. Mantyjarvi M, Tuppurainen K. Color vision in Stargardt's disease. *Int Ophthalmol*. 1992;16:423–428.
7. Tanna P, Strauss RW, Fujinami K, Michaelides M. Stargardt disease: clinical features, molecular genetics, animal models and therapeutic options. *Br J Ophthalmol*. 2017;101:25–30.
8. Fishman GA, Farbman JS, Alexander KR. Delayed rod dark adaptation in patients with Stargardt's disease. *Ophthalmology*. 1991;98:957–962.
9. Fishman GA, Farber M, Patel BS, Derlacki DJ. Visual acuity loss in patients with Stargardt's macular dystrophy. *Ophthalmology*. 1987;94:809–814.
10. Allikmets R, Singh N, Sun H, et al. A photoreceptor cell-specific ATP-binding transporter gene (ABCR) is mutated in recessive Stargardt macular dystrophy. *Nat Genet*. 1997;15:236–246.
11. Illing M, Molday LL, Molday RS. The 220-kDa rim protein of retinal rod outer segments is a member of the ABC transporter superfamily. *J Biol Chem*. 1997;272:10303–10310.
12. Rivera A, White K, Stohr H, et al. A comprehensive survey of sequence variation in the ABCA4 (ABCR) gene in Stargardt disease and age-related macular degeneration. *Am J Hum Genet*. 2000;67:800–813.
13. Schulz HL, Grassmann F, Kellner U, et al. Mutation spectrum of the ABCA4 gene in 335 Stargardt disease patients from a multicenter german cohort-impact of selected deep intronic variants and common SNPs. *Invest Ophthalmol Vis Sci*. 2017;58:394–403.
14. Cremers FP, van de Pol DJ, van Driel M, et al. Autosomal recessive retinitis pigmentosa and cone-rod dystrophy caused by splice site mutations in the Stargardt's disease gene ABCR. *Hum Mol Genet*. 1998;7:355–362.
15. Nasonkin I, Illing M, Koehler MR, Schmid M, Molday RS, Weber BH. Mapping of the rod photoreceptor ABC transporter (ABCR) to 1p21-p22.1 and identification of novel mutations in Stargardt's disease. *Hum Genet*. 1998;102:21–26.
16. Fishman GA, Stone EM, Eliason DA, Taylor CM, Lindeman M, Derlacki DJ. ABCA4 gene sequence variations in patients with autosomal recessive cone-rod dystrophy. *Arch Ophthalmol*. 2003;121:851–855.
17. Klevering BJ, Blankenagel A, Maugeri A, Cremers FP, Hoyng CB, Rohrschneider K. Phenotypic spectrum of autosomal recessive cone-rod dystrophies caused by mutations in the ABCA4 (ABCR) gene. *Invest Ophthalmol Vis Sci*. 2002;43:1980–1985.
18. Lee W, Schuerch K, Zernant J, et al. Genotypic spectrum and phenotype correlations of ABCA4-associated disease in patients of south Asian descent. *Eur J Hum Genet*. 2017;25:735–743.
19. Zernant J, Lee W, Collison FT, et al. Frequent hypomorphic alleles account for a significant fraction of ABCA4 disease and distinguish it from age-related macular degeneration. *J Med Genet*. 2017;54:404–412.
20. Cornelis SS, Bax NM, Zernant J, et al. In silico functional meta-analysis of 5,962 ABCA4 variants in 3,928 retinal dystrophy cases. *Hum Mutat*. 2017;38:400–408.
21. Sun H, Nathans J. Stargardt's ABCR is localized to the disc membrane of retinal rod outer segments. *Nat Genet*. 1997;17:15–16.
22. Molday LL, Rabin AR, Molday RS. ABCR expression in foveal cone photoreceptors and its role in Stargardt macular dystrophy. *Nat Genet*. 2000;25:257–258.
23. Quazi F, Lenevich S, Molday RS. ABCA4 is an N-retinylidene-phosphatidylethanolamine and phosphatidylethanolamine importer. *Nat Commun*. 2012;3:925.
24. Quazi F, Molday RS. ATP-binding cassette transporter ABCA4 and chemical isomerization protect photoreceptor cells from the toxic accumulation of excess 11-cis-retinal. *Proc Natl Acad Sci U S A*. 2014;111:5024–5029.
25. Sun H, Molday RS, Nathans J. Retinal stimulates ATP hydrolysis by purified and reconstituted ABCR, the photoreceptor-specific ATP-binding cassette transporter responsible for Stargardt disease. *J Biol Chem*. 1999;274:8269–8281.

26. Beharry S, Zhong M, Molday RS. N-retinylidene-phosphatidylethanolamine is the preferred retinoid substrate for the photoreceptor-specific ABC transporter ABCA4 (ABCR). *J Biol Chem*. 2004;279:53972–53979.
27. Weng J, Mata NL, Azarian SM, Tzekov RT, Birch DG, Travis GH. Insights into the function of rim protein in photoreceptors and etiology of Stargardt's disease from the phenotype in *abcr* knockout mice. *Cell*. 1999;98:13–23.
28. Boyer NP, Higbee D, Currin MB, et al. Lipofuscin and N-retinylidene-N-retinylethanolamine (A2E) accumulate in retinal pigment epithelium in absence of light exposure: their origin is 11-cis-retinal. *J Biol Chem*. 2012;287:22276–22286.
29. Molday RS, Zhong M, Quazi F. The role of the photoreceptor ABC transporter ABCA4 in lipid transport and Stargardt macular degeneration. *Biochim Biophys Acta*. 2009;1791:573–583.
30. Sparrow JR, Boulton M. RPE lipofuscin and its role in retinal pathobiology. *Exp Eye Res*. 2005;80:595–606.
31. Rozet JM, Gerber S, Ghazi I, et al. Mutations of the retinal specific ATP binding transporter gene (ABCR) in a single family segregating both autosomal recessive retinitis pigmentosa RP19 and Stargardt disease: evidence of clinical heterogeneity at this locus. *J Med Genet*. 1999;36:447–451.
32. Lewis RA, Shroyer NF, Singh N, et al. Genotype/phenotype analysis of a photoreceptor-specific ATP-binding cassette transporter gene, ABCR, in Stargardt disease. *Am J Hum Genet*. 1999;64:422–434.
33. Klevering BJ, van Driel M, van de Pol DJ, Pinckers AJ, Cremers FP, Hoyng CB. Phenotypic variations in a family with retinal dystrophy as result of different mutations in the ABCR gene. *Br J Ophthalmol*. 1999;83:914–918.
34. Sun H, Smallwood PM, Nathans J. Biochemical defects in ABCR protein variants associated with human retinopathies. *Nat Genet*. 2000;26:242–246.
35. Wiszniewski W, Zaremba CM, Yatsenko AN, et al. ABCA4 mutations causing mislocalization are found frequently in patients with severe retinal dystrophies. *Hum Mol Genet*. 2005;14:2769–2778.
36. Zhang N, Tsybovsky Y, Kolesnikov AV, et al. Protein misfolding and the pathogenesis of ABCA4-associated retinal degenerations. *Hum Mol Genet*. 2015;24:3220–3237.
37. Rosenberg T, Klie F, Garred P, Schwartz M. N965S is a common ABCA4 variant in Stargardt-related retinopathies in the Danish population. *Mol Vis*. 2007;13:1962–1969.
38. Cideciyan AV, Swider M, Aleman TS, et al. ABCA4 disease progression and a proposed strategy for gene therapy. *Hum Mol Genet*. 2009;18:931–941.
39. Kim LS, Fishman GA. Comparison of visual acuity loss in patients with different stages of Stargardt's disease. *Ophthalmology*. 2006;113:1748–1751.
40. Fishman GA. Fundus flavimaculatus. A clinical classification. *Arch Ophthalmol*. 1976;94:2061–2067.
41. Zhong M, Molday LL, Molday RS. Role of the C terminus of the photoreceptor ABCA4 transporter in protein folding, function, and retinal degenerative diseases. *J Biol Chem*. 2009; 284:3640–3649.
42. MacKenzie D, Arendt A, Hargrave P, McDowell JH, Molday RS. Localization of binding sites for carboxyl terminal specific anti-rhodopsin monoclonal antibodies using synthetic peptides. *Biochemistry*. 1984;23:6544–6549.
43. Garwin GG, Saari JC. High-performance liquid chromatography analysis of visual cycle retinoids. *Methods Enzymol*. 2000;316:313–324.
44. Zhong M, Molday RS. Binding of retinoids to ABCA4, the photoreceptor ABC transporter associated with Stargardt macular degeneration. *Methods Mol Biol*. 2010;652:163–176.
45. Ahn J, Beharry S, Molday LL, Molday RS. Functional interaction between the two halves of the photoreceptor-specific ATP binding cassette protein ABCR (ABCA4). Evidence for a non-exchangeable ADP in the first nucleotide binding domain. *J Biol Chem*. 2003;278:39600–39608.
46. Bungert S, Molday LL, Molday RS. Membrane topology of the ATP binding cassette transporter ABCR and its relationship to ABC1 and related ABCA transporters: identification of N-linked glycosylation sites. *J Biol Chem*. 2001;276:23539–23546.
47. Ahn J, Wong JT, Molday RS. The effect of lipid environment and retinoids on the ATPase activity of ABCR, the photoreceptor ABC transporter responsible for Stargardt macular dystrophy. *J Biol Chem*. 2000;275:20399–20405.
48. Qian H, Zhao X, Cao P, Lei J, Yan N, Gong X. Structure of the human lipid exporter ABCA1. *Cell*. 2017;169:1228–1239.e1210.
49. Maugeri A, van Driel MA, van de Pol DJ, et al. The 2588G–>C mutation in the ABCR gene is a mild frequent founder mutation in the Western European population and allows the classification of ABCR mutations in patients with Stargardt disease. *Am J Hum Genet*. 1999;64:1024–1035.
50. Michaelides M, Chen LL, Brantley MA Jr, et al. ABCA4 mutations and discordant ABCA4 alleles in patients and siblings with bull's-eye maculopathy. *Br J Ophthalmol*. 2007; 91:1650–1655.
51. Molday LL, Wahl D, Sarunic MV, Molday RS. Localization and functional characterization of the p.Asn965Ser (N965S) ABCA4 variant in mice reveal pathogenic mechanisms underlying Stargardt macular degeneration. *Hum Mol Genet*. 2018;27:295–306.
52. Burke TR, Fishman GA, Zernant J, et al. Retinal phenotypes in patients homozygous for the G1961E mutation in the ABCA4 gene. *Invest Ophthalmol Vis Sci*. 2012;53:4458–4467.
53. Sangermano R, Bax NM, Bauwens M, et al. Photoreceptor progenitor mRNA analysis reveals exon skipping resulting from the ABCA4 c.5461–10T–>C mutation in Stargardt disease. *Ophthalmology*. 2016;123:1375–1385.
54. Sangermano R, Khan M, Cornelis SS, et al. ABCA4 midigenes reveal the full splice spectrum of all reported noncanonical splice site variants in Stargardt disease. *Genome Res*. 2018;28: 100–110.
55. Rozet JM, Gerber S, Souied E, et al. Spectrum of ABCR gene mutations in autosomal recessive macular dystrophies. *Eur J Hum Genet*. 1998;6:291–295.
56. Chacon-Camacho OF, Granillo-Alvarez M, Ayala-Ramirez R, Zenteno JC. ABCA4 mutational spectrum in Mexican patients with Stargardt disease: identification of 12 novel mutations and evidence of a founder effect for the common p.A1773V mutation. *Exp Eye Res*. 2013;109:77–82.
57. Sciezynska A, Ozieblo D, Ambroziak AM, et al. Next-generation sequencing of ABCA4: high frequency of complex alleles and novel mutations in patients with retinal dystrophies from Central Europe. *Exp Eye Res*. 2015;145:93–99.
58. Duno M, Schwartz M, Larsen PL, Rosenberg T. Phenotypic and genetic spectrum of Danish patients with ABCA4-related retinopathy. *Ophthalmic Genet*. 2012;33:225–231.

Investigative Ophthalmology & Visual Science